Mammary glands of adipophilin-null mice produce an amino-terminally truncated form of adipophilin that mediates milk lipid droplet formation and secretion

Tanya D. Russell,[1,*,†] Carol A. Palmer,[1,§] David J. Orlicky,[**] Elise S. Bales,[†] Benny Hung-Junn Chang,[††] Lawrence Chan,[††] and James L. McManaman[2,*,†,§]

Graduate Program in Molecular Biology,* Division of Basic Reproductive Science, Department Obstetrics and Gynecology,† Department of Physiology and Biophysics,§ and Department of Pathology,** University of Colorado at Denver and Health Sciences Center, Aurora, CO; and Department of Molecular and Cellular Biology and Division of Diabetes, Endocrinology, and Metabolism, Department of Medicine,†† Baylor College of Medicine, Houston, TX

Abstract **Adipophilin (ADPH), a member of the perilipin family of lipid droplet-associated proteins, is hypothesized to mediate milk lipid formation and secretion. Unexpectedly, the fat content of milk from ADPH-null mice was only modestly lower than that of wild-type controls, and neither TIP47 nor perilipin appeared to fully compensate for ADPH loss. This prompted us to investigate the possibility that the mutated ADPH gene was not a genuine null mutation. ADPH transcripts were detected in ADPH-null mammary tissue by quantitative real-time PCR, and C-terminal-specific, but not N-terminal-specific, ADPH antibodies detected a single lower molecular weight product and immunostained cytoplasmic lipid droplets (CLDs) and secreted milk fat globules in ADPH-null mammary tissue. Furthermore, stable cell lines expressing cDNA constructs corresponding to the ADPH-null mutation produced a product comparable in size to the one detected in ADPH-null mammary glands and localized to CLDs. Based on these data, we conclude that ADPH-null mice express an N-terminally truncated form of ADPH that retains the ability to promote the formation and secretion of milk lipids.**—Russell, T. D., C. A. Palmer, D. J. Orlicky, E. S. Bales, B. H-J. Chang, L. Chan, and J. L. McManaman. **Mammary glands of adipophilin-null mice produce an amino-terminally truncated form of adipophilin that mediates milk lipid droplet formation and secretion. *J. Lipid Res.* 2008.** 49: **206–216.**

Supplementary key words PAT domain • functional differentiation • TIP47 compensation

A large body of evidence suggests that proteins located on the surface of cytoplasmic lipid droplets (CLDs) play important roles in lipid storage, trafficking, and secretion (1, 2). Although the physiological roles of apolipoproteins in the formation and secretion of lipoprotein particles are well established, much less is known about the proteins and processes that mediate CLD formation and secretion. The PAT (for perilipin, adipophilin, and TIP47) family of CLD-associated proteins are attractive candidates as regulators of lipid storage and secretion in the mammary gland (3–5). Perilipin expression appears to be limited to adipose and steroidogenic tissue (6), whereas adipophilin (ADPH) and TIP47 are ubiquitously expressed in a wide range of tissue types (7–9). TIP47 was originally coidentified as a 48 kDa placental protein 17b, or PP17b (10, 11), and an endosomal trafficking guide for mannose 6-phosphate receptors (12); however, subsequent studies have demonstrated that it can also bind to CLD (13). In addition, it has been reported to be associated with milk fat globules in human milk (14). ADPH is hypothesized to play a key role in CLD formation: it localizes to CLDs in many mammalian cell types, including mammary epithelial cells (5, 7, 8, 15, 16), and cellular levels of ADPH have been shown to correlate with lipid accumulation in a variety of cells and tissues (17–23). We have shown that ADPH is selectively expressed by secretory epithelial cells in the mouse mammary gland and that its expression is developmentally linked to CLD accumulation during the differentiation of the mammary gland into a secretory organ during the last half of pregnancy (5). Evidence of functional redundancy among members of the PAT family in CLD formation and metabolism (24, 25) further underscores the importance of these proteins in CLD function. The lactating mammary gland continuously generates and secretes CLDs, and lipids are a substantial component of the milk of most species; for this reason, this system provides a sensitive physiological model to investigate the regulation of CLD formation and secretion.

Manuscript received 4 September 2007 and in revised form 3 October 2007.

Published, JLR Papers in Press, October 5, 2007.
DOI 10.1194/jlr.M700396-JLR200

[1] T. D. Russell and C. A. Palmer contributed equally to this study.
[2] To whom correspondence should be addressed.
e-mail: jim.mcmanaman@uchsc.edu

In many species, including mice, the lactating mammary gland is one of the most active lipogenic organs in the body (26, 27). The mouse mammary gland is a particularly ideal model because most of its development occurs after birth. Specifically, pubertal hormones stimulate the formation of tree-like ductal structures that extend from the nipple into the mammary fat pad (28). The milk-secreting units, called alveoli, originate from these structures; they grow and mature during pregnancy into grape-like clusters of epithelial cells that, at parturition, become highly secretory (29). These cells actively produce and secrete lipids into the alveolar lumina by a distinct multistep process. Milk lipids originate from triglycerides and cholesteryl esters synthesized by endoplasmic reticulum-associated enzymes and are released into the cytoplasm as protein-coated CLDs (4). In a unique secretion process, the CLDs move toward the apical membrane, contacting and becoming progressively enveloped by this structure (3, 30) before being released into the lumina as membrane-coated structures known as milk fat globules. Despite the nutritional importance of milk lipids and the prominence of lipid biogenesis and secretion in the function of alveolar epithelial cells, the factors regulating the formation and secretion of CLDs remain poorly defined.

In this study, we use the differentiating mammary gland to test the hypothesis that ADPH regulates CLD formation, accumulation, and secretion by comparing these processes in wild-type (WT) mice and mice believed to lack ADPH (31). Our results show that CLD accumulated in secretory epithelial cells during the differentiation of mammary glands of putative ADPH-null mice and that the milk fat content of these mice was only modestly lower than that of WT mice. In the course of characterizing the basis for the modest lactation phenotype observed in ADPH-null animals, we found that these mice express an N-terminally truncated form of ADPH that may play a role in milk lipid formation. Possible compensatory functional roles of truncated ADPH and TIP47 in the accumulation and secretion of CLD are investigated in differentiating and lactating mouse mammary tissue.

MATERIALS AND METHODS

Animals and tissue preparation

B6.129-Adfp^{tm1Chan} mice deficient in ADPH were generated as described previously (31). WT C57B6 mice were obtained from Jackson Laboratories. Both strains were maintained as breeding colonies in the Animal Resource Center of the University of Colorado Health Sciences Center (UCHSC) and housed individually. Pregnancy was timed by the observation of vaginal plugs after mating. The first day of pregnancy was taken as the day of vaginal plug detection. Parturition occurs on approximately day 19 of pregnancy; the day of birth is also designated as day 1 of lactation. Mammary tissue was removed from animals euthanized by carbon dioxide at the times indicated in the text and flash-frozen in liquid nitrogen or processed for immunofluorescence microscopy (5, 32). All animal procedures were approved by the Institutional Animal Care and Use Committee of the UCHSC.

Antibodies

Antibodies to amino acids 1–25 of murine ADPH (N-terminal-specific ADPH antibodies) were generated in rabbits (5) or were obtained commercially (guinea pig anti-ADPH; Research Diagnostics, Inc./Fitzgerald Industries International, Flanders NJ). Antibodies to amino acids 409–425 of murine ADPH (C-terminal-specific ADPH antibodies) were generated in rabbits (Global Peptides, Fort Collins, CO). Antibodies to amino acids 1–16 of murine TIP47 (Affinity Bioreagents, Golden, CO) were described previously (5). Guinea pig antibodies to perilipin were obtained commercially (Research Diagnostics/Fitzgerald Industries). The specificities of ADPH and TIP47 antibodies were established by competition assays using specific immunizing peptides in both Western blot and immunofluorescence assays and by the absence of reaction of anti-ADPH and anti-TIP47 with purified recombinant mouse TIP47 and ADPH proteins, respectively, using Western analysis (data not shown).

Protein extraction and immunoblot analysis

Mammary tissue was ground under liquid nitrogen using a mortar and pestle and extracted by methanol/chloroform as described previously (5). Precipitated protein was rinsed with methanol, dried, suspended in 10% SDS solution, and stored at −80°C before use. Proteins (10 μg) from mammary gland extracts were separated on 10% polyacrylamide gels and transferred to nitrocellulose membranes. ADPH was detected using either rabbit or guinea pig anti-ADPH at 1:1,000 dilution. TIP47 was detected using rabbit anti-TIP47 at 1:2,000 dilution. Corresponding horseradish peroxidase-conjugated secondary antibodies (Sigma Chemical Co., St. Louis, MO) were used according to the manufacturer's specifications. Western Lightening Chemiluminescence Reagent (Perkin-Elmer, Boston, MA) was used to detect bands, and band intensities were quantified by densitometry (ChemiDoc system; Bio-Rad, Hercules, CA). Protein standards were used at varying dilutions to verify that the densitometry responses of each protein were in the linear range.

Isolation and quantification of mRNA

Total RNA was extracted from frozen tissue using Trizol (Life Technologies) according to the manufacturer's instructions. The purity, concentration, and integrity of total RNA from each sample were verified using a NanoDrop spectrophotometer (NanoDrop Technologies, Wilmington, DE) and the RNA 6000 Nano Assay (Agilent Technologies, Palo Alto, CA) in the UCHSC Cancer Core. ADPH and TIP47 transcript copy numbers were determined by quantitative real-time (QRT)-PCR analysis using a multiplexing strategy to provide an internal standard for normalization (β_2-microglobulin). QRT-PCR assays were performed in the Quantitative Genomics Core Laboratory at the University of Texas Health Sciences Center. Primers and probes are listed in **Table 1**. All QRT-PCR assays used were validated at the Quantitative Genomics Core Laboratory to ensure that they passed the minimum requirements for efficiency, sensitivity, and selectivity. At least three tissue replicates at each time point were analyzed at least twice with similar results.

Cell lines

Plasmids containing cDNA encoding full-length murine ADPH with a C-terminal vesicular stomatitis virus glycoprotein (VSVG) epitope (pADPH[FL]VSV) were described previously (33). Plasmids containing cDNA encoding an open reading frame similar to that of ADPH Δ2,3 mice with a C-terminal VSVG epitope tag were generated by PCR amplification of pADPH[FL]VSV using forward (5′-TAAAGCTTATTGCGGTTGCCAATACCTAT-3′) and

TABLE 1. Quantitative real-time PCR primers and probes

Adipophilin	Forward	5′-CAG CCA ACG TCC GAG ATT G-3′
	Reverse	5′-CAC ATC CTT CGC CCC AGT T-3′
	Probe	5′-FAM/TGC CAG TGC CAG AGG TGC CG-3′
	Amplicon	5′-CAG CCA ACG TCC GAG ATT GTT GCC AGT GCC AGA GGT GCC GTA ACT GGG GCG AAG GAT GTG-3′
TIP47	Forward	5′-CTC AAG CTG CTA TGG AGG AAC C-3′
	Reverse	5′-CAT ACG TGG AAC TGA TAA GAG GCA-3′
	Probe	5′-56/FAM/CGT GGT GGA TCG TGT TGC CGG CGG/36-TAMSp-3′
	Amplicon	5′-AAC TCA AGC TGC TAT GGA GGA ACC TGT TGT GCA GCC CAG CGT GGT GGA TCG TGT TGC CGG CCT GCC TCT TAT CAG TTC CAC GTA TGA A-3′
B_2-microglobulin	Forward	5′-GAG CAC ATG TCT CGA TCC CAG TAG-3′
	Reverse	5′-CAT ACG CCT GC A GAG TT A AGC A-3′
	Probe	5′-HEX/AGT ATG GCC GAG CCC GAG ACC G-3′
	Amplicon	5′-AAC ATA CGC CTG CAG AGT TAA GCA TGC CAG TAT GGC CGA GCC CAA GAC CGT CTA CTG GGA TCG AGA CAT GTG ATC AA-3′

reverse (5′-GATGTCGACCTATAGAATAGGGCCCTC-3′) primers containing *Hind*III (underlined in the forward primer) and *Sal*I (underlined in the reverse primer) restriction sites. The product was cut with *Hind*III and *Sal*I and ligated into pcDNA3 that was opened with *Hind*III and *Xho*I. The resulting plasmid (pADPH[76-425]VSV) was verified to encode the carboxy-end, VSV epitope-tagged open reading frame of murine ADPH from amino acids 76 to 425 by sequence analysis. pADPH[FL]VSV and pADPH[76-425]VSV were transfected into HEK293 cells using calcium phosphate (33). Transfected cells were selected with G418 (50 μg/ml) and cloned by limiting dilution through two rounds and cultured in DMEM containing high glucose and supplemented with 6% bovine calf serum. Immunolocalization studies were carried out in cultures incubated in medium containing 300 μM oleic acid.

Immunofluorescence microscopy

Freshly dissected mouse mammary tissue was fixed by overnight incubation in neutral buffered saline and embedded in paraffin at the UCHSC Pathology Core facility. Microtome sections (8 μm) were mounted on glass slides, deparaffinized and hydrated, and subjected to antigen retrieval (Vector Laboratories) as described previously (32). The sections were then permeabilized in 0.2% glycine in PBS, blocked with 5% normal goat serum and 0.1% (w/v) saponin in PBS overnight at 4°C, and incubated with primary antibodies at the following dilutions for 1 h at room temperature: C-terminal-specific ADPH, 1:100; rabbit or guinea pig N-terminal-specific ADPH, 1:100; TIP47, 1:200; and perilipin, 1:100. Immunolabeled proteins were detected with Alexa Fluor® 594-labeled donkey anti-rabbit IgG or donkey anti-guinea pig IgG (Invitrogen/Molecular Probes, Carlsbad, CA). The luminal borders of mammary alveoli were identified by staining with Alexa Fluor® 488 conjugated to wheat germ agglutinin (Invitrogen/Molecular Probes), and nuclei were identified by 4′,6-diamidino-2-phenylindole staining as described (5).

Cultured cells, grown on glass coverslips, were fixed in 3.7% formalin for 10 min, extracted with 50% ethanol for 4 min, and washed in PBS for 30 min. Expressed forms of ADPH were detected by labeling with mouse anti-VSVG antibodies (1 μg/ml) in conjunction with Alexa Fluor® 594-labeled secondary antibodies (Invitrogen/Molecular Probes). Nuclei were stained with 4′,6-diamidino-2-phenylindole.

Digital confocal images were captured on a Nikon Eclipse 80i microscope, equipped with a RETIGA 2000R Fast cooled video camera and Nomarski optics, using a 60× objective and NIS Elements imaging software. Fluorescent images were digitally deconvolved using the No Neighbors algorithm and converted to TIFF files.

RESULTS

Loss of ADPH decreases milk fat

The functional importance of ADPH in the formation and secretion of milk lipids was initially investigated by comparing milk fat content from WT and ADPH-null mice. At midlactation [postcoital day (PCD) 29], the fat content (vol%) of milk from ADPH -null mice (24.2 ± 1.7%) was 12% lower than that of WT mice (27.4 ± 1.1%). Although this difference is statistically significant ($P < 0.0001$; n = 10), these data suggested that either ADPH has only a modest role in the production and/or secretion of milk lipids or another protein compensated for ADPH in these processes. Because TIP47 is structurally similar to ADPH (34), we hypothesized that it could functionally compensate for ADPH with regard to lipid droplet formation and secretion in mammary epithelial cells.

TIP47 replaces ADPH on CLDs in ADPH-null mice

In previous studies, TIP47 was shown to substitute for ADPH in the formation of CLDs in fibroblasts from ADPH-null mice (25). To determine whether other PAT proteins substitute for ADPH in milk lipid formation and/or secretion in ADPH-null mice, we immunostained mammary gland sections from WT and ADPH-null mice for ADPH, TIP47, and perilipin (**Fig. 1**). In agreement with previous studies (5), ADPH immunostaining specifically localized to CLDs in secretory epithelial cells of WT mammary glands (Fig. 1A, panel a), whereas TIP47 staining was detected as diffusely distributed punctate structures (Fig. 1A, panel b) and perilipin staining was restricted to a few small islands of lipid-depleted adipose tissue that remain in the mammary gland during lactation (Fig. 1A, panel c). As expected, we did not detect ADPH immunostaining in mammary glands of ADPH-null mice using

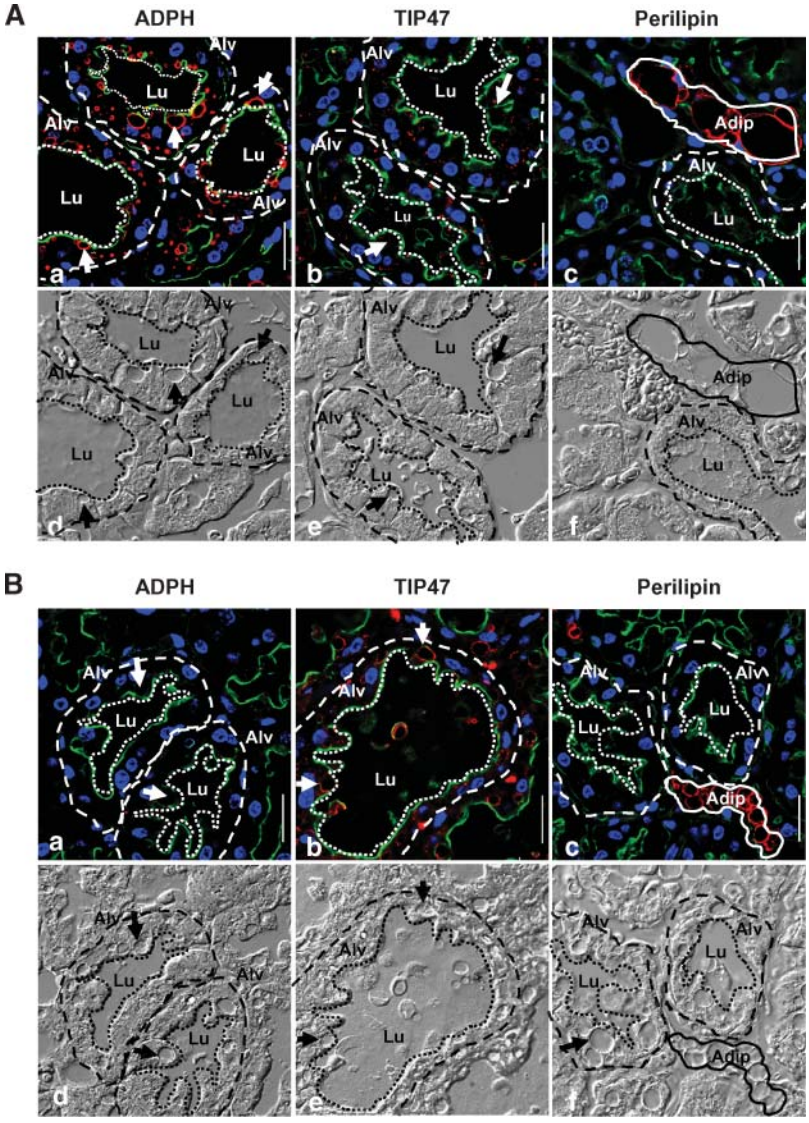

Fig. 1. TIP47 associates with cytoplasmic lipid droplet (CLDs) in adipophilin (ADPH)-null mice. Immunolocalization of ADPH, TIP47, and perilipin in lactating [day 10, postcoital day (PCD) 29] mammary glands of wild-type (WT; A) and ADPH-null (B) mice using antibodies against the N-terminus of mouse ADPH (a), TIP47 (b), or perilipin (c) and Alexa 594 (red)-conjugated secondary antibodies. Corresponding Nomarski images (d–f) denote structural features of immunostained sections. For ease of identification, some alveoli (Alv) are outlined by dashed lines. Luminal borders of mammary alveoli were identified by staining with Alexa 488-conjugated wheat germ agglutinin (green) and are indicated by dotted lines. Lu indicates the luminal area of alveoli. Adipose tissue (Adip) is outlined by solid lines (c, f). Arrows in immunostained and Nomarski images indicate CLDs in mammary alveoli. Note that CLDs in alveoli of WT mice are positive for ADPH (white arrows; A, panel a) and negative for TIP47 (white arrows; A, panel b), whereas they are negative for ADPH (white arrows; B, panel a) and positive for TIP47 (white arrows, B, panel b) in alveoli of ADPH-null mice. Perilipin localizes exclusively to mammary adipose in both WT and ADPH-null mice (A, B, panel c). Bars = 50 μm.

N-terminal-specific ADPH antibodies (Fig. 1B, panel a). However, in contrast to WT glands, TIP47-positive CLDs were detected in secretory epithelial cells of ADPH-null mice (Fig. 1B, panel b), although the staining was patchy and some CLDs did not appear to possess TIP47. As in WT mice, perilipin staining was detected only in adipose tissue in mammary glands of ADPH-null mice. These results are consistent with the findings of Sztalryd et al. (25) in fibroblasts, showing that TIP47 localizes to CLDs in ADPH-deficient mice, and raise the possibility that it might substitute for ADPH in milk lipid formation and secretion in ADPH-null mice. However, the patchy TIP47 staining pattern and the absence of TIP47 from some CLDs raised questions about its role in these processes.

Developmental TIP47 expression in ADPH-null mice

ADPH expression has been shown to be closely linked to CLD accumulation in differentiating mammary glands

of WT mice (5). We hypothesized that there would be a compensatory increase of TIP47 expression to correlate with these processes in ADPH-null mice. The size and number of CLDs in secretory epithelial cells in the mouse mammary gland have been shown previously to increase dramatically in conjunction with alveolar differentiation during late pregnancy and then to decrease once lactation is initiated after parturition (5). We obtained similar results in the ADPH-null mouse; confocal microscopy using Nomarski optics (**Fig. 2A**, panels e–h) shows that by PCD 18 (the day before parturition in our colony), the cytoplasm of alveolar epithelial cells is filled with large CLDs, often with diameters in excess of 10 μm (Fig. 2A, panel f). Within 24 h after parturition (PCD 20), secretory epithelial cells contained smaller CLDs, many of which were observed to be adjacent to the apical border (Fig. 2A, panel g). Immunofluorescence analysis of these sections showed intense TIP47 staining of CLDs in secretory epithelial cells at PCD 18 (Fig. 2A, panel b). However, by PCD 20, the staining was less prominent and many CLDs were not positive for TIP47 (Fig. 2A, panel c). By midlactation (PCD 29), relatively few CLDs stained for TIP47 (Fig. 2A, panel d).

To determine whether TIP47 staining of CLDs correlates with its tissue levels, we characterized TIP47 protein and mRNA levels in mammary glands of differentiating and lactating ADPH-null mice. Figure 2B shows that relative TIP47 protein levels in ADPH-null animals increased ~6-fold between PCD 10 and PCD 16 and then decreased steadily, so that by PCD 29 they were ~8% of the PCD 16 values. In contrast, TIP47 protein levels in mammary glands of WT mice changed relatively little during pregnancy and increased ~6-fold between PCD 18 and PCD 29. These changes in TIP47 protein levels in both WT and ADPH-null mice appear to be mediated by translational or posttranslational processes, as mammary gland TIP47 mRNA levels were similar and increased during mammary gland differentiation and lactation in both lines of mice (Fig. 2C). These results suggest that TIP47 can associate with CLDs and that the protein level is high enough during pregnancy to associate with CLDs in the absence of WT ADPH. However, these findings and the immunocytochemistry results in Fig. 2A suggest that the protein is not directly related to lipid secretion during lactation in either WT or mutant mice.

ADPH-null mice express an N-terminally truncated form of ADPH

ADPH-null mice were generated by replacing exons 2 (which contains the translation start site) and 3 of the ADPH gene with a neo cassette, and on the basis of Northern analysis and immunoblot studies with an N-terminal antibody they were thought to be ADPH-null. However, in the process of exploring other possible explanations for relatively unaffected milk lipid formation and secretion in these mice, we noted that the disrupted ADPH gene sequence possessed a potential start site in exon 5 (**Fig. 3A**). This raised the possibility that a truncated form of ADPH might be synthesized. To test this possibility, we generated antibodies against amino acids 409–425 (the C terminus) of mouse ADPH. Figure 3B shows immunoblots of mammary gland extracts from WT and ADPH-null mice at lactation day 10 using C- and N-terminal-specific antibodies. As expected, N-terminal antibodies detected a single band at ~50 kDa in WT mammary glands but failed to detect any bands in extracts from ADPH-null mammary glands. In contrast, C-terminal antibodies detected both the 50 kDa band and a lower molecular mass band in extracts of WT mammary glands (Fig. 3B, small arrows), whereas only the lower molecular mass band was detected in extracts of ADPH-null mammary glands (a nonspecific band near 75 kDa is detected in some extracts). Immunofluorescence analysis (Fig. 3C) verified that the C-terminal antibodies selectively stained CLDs in sections from lactating WT and ADPH-null glands and that in both cases staining was blocked by preincubating the antibodies with the immunizing peptide before staining.

To further test the possibility that a translatable product can be obtained from exons 4–8 of mouse ADPH, we stably transfected HEK293 cells, which lack endogenous ADPH (unpublished observations), with a plasmid that expresses cDNA corresponding to these exons linked at its 3′ end to the coding sequence of the 11 amino acid VSVG monoclonal antibody epitope. Immunoblot analysis of extracts of these cells (Δ2,3-ADPH-VSV) using anti-VSVG antibodies shows that they produced a single protein species of approximately the same size as the lower molecular mass form of ADPH observed in extracts of WT and ADPH-null mammary glands (Fig. 3D). Identical results were obtained using C-terminal-specific ADPH antibodies, whereas N-terminal-specific antibodies failed to detect any bands (data not shown). Immunofluorescence analysis of cells expressing the truncated form of ADPH (Fig. 3E) verified that it selectively localized to CLDs. Based on these results, the ADPH-null mutant mice appear to produce an N-terminally truncated form of ADPH that retains at least some functional properties. These mice will subsequently be referred to as Δ2,3 ADPH mice.

Truncated ADPH levels increase during mammary gland differentiation

To test the possibility that the N-terminally truncated form of APDH contributes to milk lipid formation and secretion, mammary gland sections from pregnant and lactating WT and Δ2,3 ADPH mice were stained with C-terminal-specific ADPH antibodies (**Fig. 4A**). Corroborating previous studies (5), prominent large ADPH-positive CLDs were detected in secretory epithelial cells in WT mammary glands beginning around PCD 16; they completely filled these cells by PCD 18 (Fig. 4A, top panels). During lactation, ADPH-positive CLDs were seen adjacent to apical membranes of secretory epithelial cells and in the luminal space of alveoli in WT animals soon after parturition (PCD 21) and at midlactation (PCD 29) (Fig. 4A, top panels). In contrast, ADPH-positive CLDs were not detected in secretory epithelial cells of Δ2,3 ADPH mice at PCD 16 and were seen only occasionally in these cells at PCD 18 (Fig. 4A, bottom panels). However, ADPH-positive

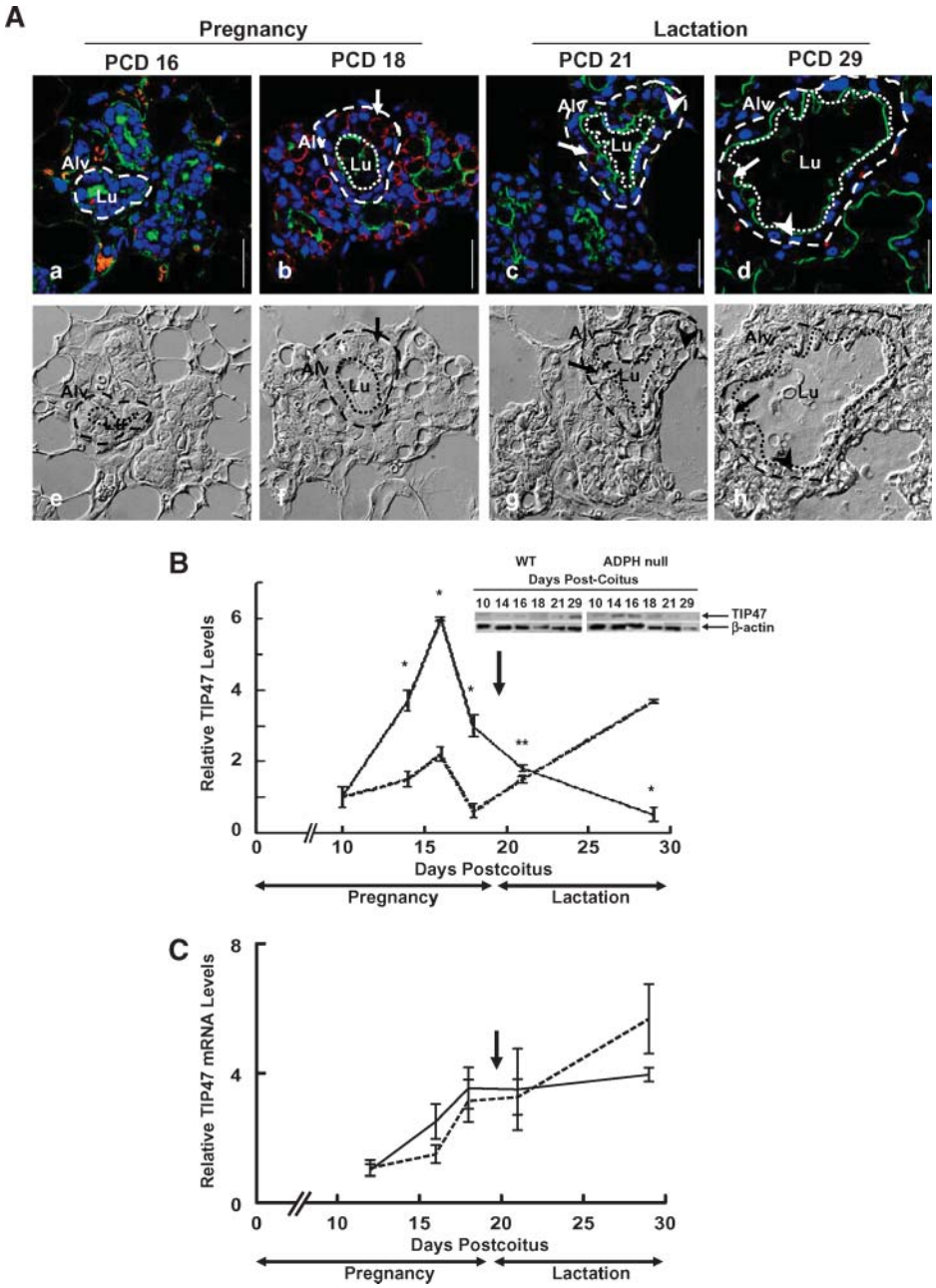

Fig. 2. TIP47 levels do not correlate with milk lipid secretion in ADPH-null mice. A: TIP47 immunostaining (red) in differentiating and lactating ADPH-null mouse mammary tissue at PCD 16 (a), PCD 18 (b), PCD 21 (lactation day 2) (c), and PCD 29 (lactation day 10) (d). Corresponding Nomarski images are shown in e–h. Intense TIP47 staining of large CLDs is observed in mammary alveoli just before parturition (arrows, PCD 18). TIP47-positive CLDs are detected in alveoli of lactating ADPH-null mice (arrows, panels c, g, d, h), but TIP47 staining intensity is reduced compared with that in late pregnant animals (panel b) and some CLDs are not TIP47-positive (arrowheads, panels c, g, d, h). Alveoli (Alv) are indicated by dashed outline; luminal areas (Lu) were identified by Alexa 488-conjugated wheat germ agglutinin staining and are indicated by dotted outline. Bars = 50 μm. B: Relative TIP47 levels in mammary tissue from differentiating and lactating WT (thick, dashed line) and ADPH-null (thin, solid line) mice were determined by immunoblot analysis and quantified by densitometry. The values are average ± SEM densitometric measurements normalized to β-actin from three to four animals per time point and are shown as ratios to PCD 10. * $P < 0.000001$, ** $P < 0.0005$, comparing WT and ADPH-null mice. The arrow indicates the time of parturition. Representative immunoblot analyses in the inset indicate TIP47 and β-actin levels. Immunoblot analyses of tissue extracts were performed twice with similar results. C: TIP47 mRNA expression in differentiating and lactating mammary glands of WT (thick, dashed line) and ADPH-null (thin, solid line) mice was determined by quantitative real-time (QRT)-PCR. Values are average copy numbers ± SEM normalized to average β_2-microglobulin × 100. n = 3–4 animals per time point. There was no statistically significant difference comparing WT and ADPH-null mice. The arrow indicates the time of parturition.

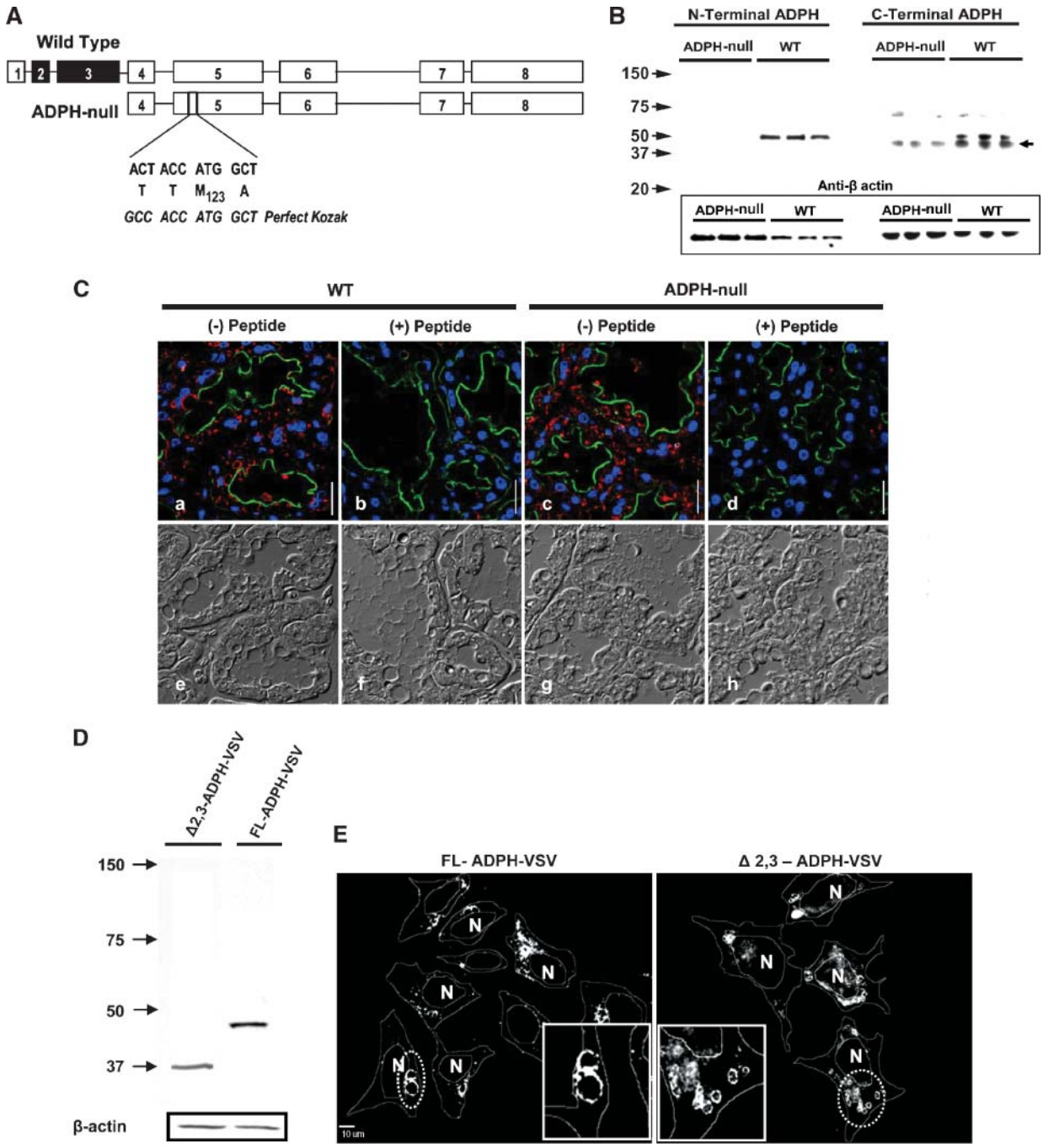

Fig. 3. ADPH-null mice produce an N-terminally truncated ADPH. A: ADPH exon organization in WT and ADPH-null mice showing the oligonucleotide and corresponding amino acid sequences of the putative alternative translation initiation site in exon 5. Black rectangles represent exons removed in ADPH-null mice. The oligonucleotide sequence of a perfect Kozak element is shown in italics. B: Immunoblot of lactating (day 10, PCD 29) mammary gland extracts with N-terminal- and C-terminal-specific antibodies to mouse ADPH. N-terminal-specific antibodies detect a single band at ~50 kDa in extracts of WT mouse mammary glands but fail to detect any bands in mammary gland extracts of ADPH-null mice. C-terminal specific-antibodies detect both the ~50 kDa band and the lower molecular mass band in WT mammary gland extracts but detect only the lower molecular mass band in extracts from ADPH-null mammary glands. The band at ~70 kDa in both WT and ADPH-null extracts is a nonspecific reaction product. The boxed region at bottom shows corresponding β-actin loading controls. C: C-terminal-specific ADPH antibodies selectively stain CLDs in mammary gland sections of day 10 lactating WT and ADPH-null mice (panels a, c). Staining is blocked by preincubating antibodies with the C-terminal peptide immunogen (panels b, d). Nomarski images corresponding to panels a–d are shown in panels e–h. Bars = 50 μm. D: Immunoblots of HEK293 cells stably transfected with plasmids expressing cDNA encoding full-length ADPH-VSV or Δ2,3 ADPH-VSV using antibodies to the VSV epitope (see Methods). Extracts of cells expressing full-length ADPH-VSV (FL-ADPH-VSV) show a single band that is ~50 kDa, whereas extracts of cells expressing Δ2,3 ADPH-VSV show a single lower molecular mass band that corresponds in size to the lower molecular mass band found in extracts of ADPH-null mammary glands. β-Actin loading controls are shown in the boxed region at bottom. E: Immunolocalization of FL-ADPH-VSV and Δ2,3 ADPH-VSV using anti-VSV antibodies show that both molecules localize to clusters of CLDs (dotted outline). Cells and nuclei (N) are outlined based on Nomarski results. Insets show enlarged CLD-positive regions in both cell lines. Bar = 10 μm.

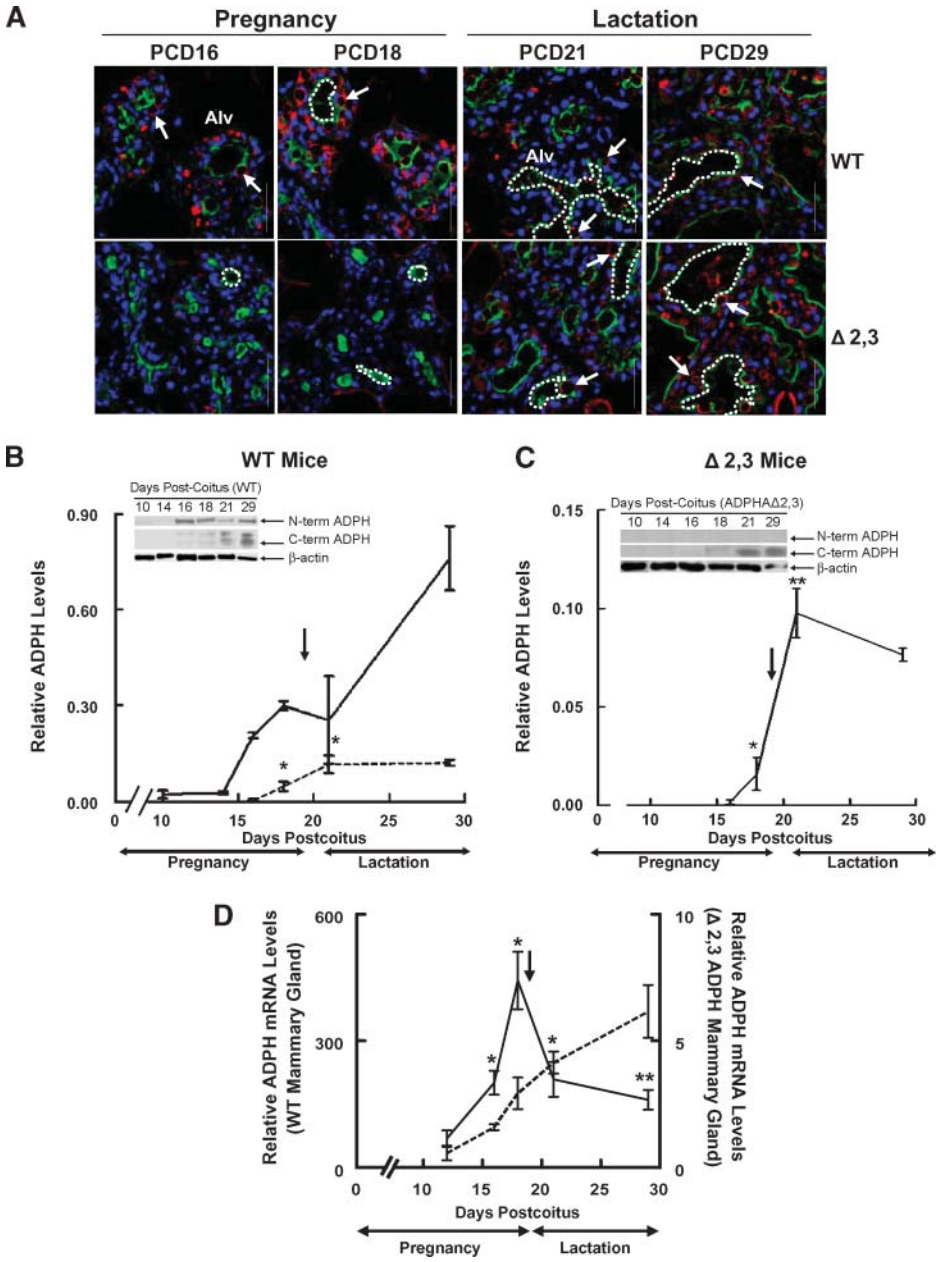

Fig. 4. Truncated ADPH expression correlates with milk lipid secretion in Δ2,3 ADPH mice. A: C-terminal ADPH immunostaining (red) in pregnant (PCD 16 and PCD 18) and lactating (PCD 21 and PCD 29) mammary tissue from WT and ADPH-null mice (Δ2,3 ADPH mice). CLDs in WT mammary glands are positive for ADPH (arrows) from PCD 16 to PCD 29. CLDs in Δ2,3 ADPH mice are not positive for ADPH until after parturition (arrows; PCD 21 to PCD 29). Alveoli (Alv) are indicated by dashed outline; luminal areas were identified by Alexa 488-conjugated wheat germ agglutinin staining. Bars = 50 μm. B: Levels of full-length (thin, solid line) and truncated (thick, dashed line) ADPH in Western blots of mammary tissue from WT mice using the C-terminal ADPH antibody. The arrow indicates the time of parturition. * $P < 0.005$ compared with PCD 10. The inset shows representative immunoblots of ADPH and β-actin. C: Truncated ADPH protein levels in mammary tissue from differentiating and lactating Δ2,3 ADPH mice. The arrow indicates the time of parturition. * $P < 0.05$, ** $P < 0.0005$ compared with PCD 10. The inset shows representative immunoblots of ADPH and β-actin. In B and C, the values are average ± SEM densitometric measurements normalized to β-actin from three to four animals per time point and are shown as ratios to PCD 10. Immunoblot analyses of tissue extracts were performed twice with similar results. D: ADPH mRNA levels in differentiating and lactating mammary glands of WT (thick, dashed line) and Δ2,3 ADPH (thin, solid line) mice were determined by QRT-PCR. Values are average copy numbers ± SEM normalized to average β_2-microglobulin × 100. n = 3–4 animals per time point. * $P < 0.0001$, ** $P < 0.001$ comparing WT and ADPH-null mice. The arrow indicates the time of parturition.

CLDs were detected in secretory epithelial cells of Δ2,3 ADPH mice after parturition (PCD 21), and numerous ADPH-positive CLDs were observed adjacent to apical membranes of secretory membranes of epithelial cells and in the luminal space of their alveoli by PCD 29, which suggests that they undergo secretion as milk fat globules. Immunoblots of differentiating and mature mammary gland tissue showed that ADPH levels correlated with the appearance of ADPH-positive CLDs in both WT mice (Fig. 4B) and Δ2,3 ADPH mice (Fig. 4C). Importantly, the timing of the appearance of truncated ADPH in mammary tissue correlates with the onset of CLD secretion in Δ2,3 ADPH mice.

To determine whether the apparent delay in the appearance of truncated ADPH in Δ2,3 ADPH mouse mammary glands was related to delayed expression, we quantified ADPH transcript levels in mammary tissue of pregnant and lactating WT and Δ2,3 ADPH mice (Fig. 4D). Using primers directed at exon boundaries 4 and 5 (Table 1), we found that ADPH transcript levels increased significantly between PCD 12 and PCD 16 in both WT and Δ2,3 ADPH mice (Fig. 4D); however, transcript levels in Δ2,3 ADPH mice were 5% or less than those of WT mice. In addition, ADPH transcript in mammary tissue of WT mice increased into lactation (Fig. 4D, left axis), whereas transcript levels in Δ2,3 ADPH mice (Fig. 4D, right axis) decreased sharply between the end of pregnancy (PCD 18) and day 2 of lactation (PCD 21) (Fig. 4D, arrow). These results indicate that the delayed appearance of truncated ADPH in Δ2,3 ADPH mammary tissue is not the result of delayed ADPH expression and further suggest that translational and/or posttranslational mechanisms contribute to the increase in the levels of truncated ADPH in lactating mammary tissue.

DISCUSSION

We provide evidence that Δ2,3 ADPH mice, which were originally thought to lack ADPH (25, 31), produce an N-terminally truncated form of ADPH that retains at least some of the functional properties of the full-length molecule. These mice were generated by replacing exons 2 and 3 of the mouse ADPH gene with a neo cassette. Based on the structure of the mouse ADPH gene (www.ensembl.org), the disrupted gene is postulated to lack the portion of the 5′ untranslated region encoded by exon 2 and nucleotides encoding amino acids 1–75, but it may retain promoter elements and the 5′ untranslated region encoded by exon 1 as well as exons 4–8. It was originally concluded, using Northern analysis and immunoblotting with N-terminal-specific ADPH antibodies, that the disrupted gene failed to produce ADPH transcripts or a translated product (25, 31). However, our QRT-PCR analysis of mammary tissue using primers targeted to the exon 4–5 boundary of mouse ADPH shows that ADPH transcripts are present and that their levels are influenced by the developmental status of the mammary gland. These findings were confirmed by RT-PCR analysis with primers directed at exons 4 and 5 (data not shown) and indicate that the neo-disrupted ADPH gene retains the ability to undergo regulated transcription. Nevertheless, the observation that ADPH transcript levels in Δ2,3 ADPH mammary tissues are only a fraction of those in WT tissue suggests that ADPH expression is markedly reduced in Δ2,3 ADPH mice. At present, studies are under way to determine whether this reduction is attributable to diminished transcriptional efficiency of the mutated gene or decreased transcript stability.

The conclusion that neo-disrupted ADPH gene transcripts are translated is based on observations that C-terminal-specific ADPH antibodies detect a lower molecular mass band of similar size in extracts of Δ2,3 ADPH mouse mammary glands (Fig. 3B) and HEK293 cells expressing cDNA corresponding to exons 4–8 of mouse ADPH (Fig. 3C). Importantly, the cDNA construct used for our cell culture studies was generated to exactly match the sequence corresponding to exons 4–8 and therefore was constructed without an initiating ATG start site. Thus, any product generated from this construct had to be initiated from an internal start site. Although the position of the initiating methionine was not identified, translation appears to be initiated from a single site, because only a single lower molecular mass product is observed in both mammary tissue and cell culture extracts. Inspection of exons 4–8 for possible start sites showed that only the ATG encoding methionine 123 in exon 5 appeared to resemble a Kozak element (35). However, other potential ATG sequences are present in exons 4–8, and efforts are currently under way to identify the position of the initiating methionine.

Use of the antibody to the C terminus of ADPH indicates that WT mammary tissue possesses a lower molecular mass form of ADPH that is similar in size to the forms found in extracts of Δ2,3 ADPH mammary tissue and Δ2,3 ADPH cells. This observation corroborates earlier data from our laboratory demonstrating the presence of a single lower molecular mass form of ADPH by mass spectrometry on CLDs isolated from lactating WT mouse mammary alveoli and in the membrane fraction from secreted fat globules (15). Our present data indicate that this truncated form of ADPH does not appear until late pregnancy in WT and Δ2,3 ADPH mice and that its appearance lags behind the appearance of both full-length ADPH protein and ADPH transcripts. Although it is possible that the lower molecular mass form is a proteolytic product of full-length ADPH, the presence of a possible translation initiation site in exon 5 raises the intriguing possibility that it represents an alternatively translated product whose expression is regulated differently from that of the full-length product. This notion is further supported by the observation that the lower molecular mass form was not associated with CLDs isolated from liver tissue (15).

The possibility that truncated ADPH contributes to CLD formation and secretion in lactating Δ2,3 ADPH mice is suggested by our immunofluorescence data showing that it localizes to CLDs in both secretory epithelial cells and secreted milk fat globules in lactating Δ2,3 ADPH mice (Figs. 3C, 4A) as well as to CLDs in Δ2,3 ADPH cells (Fig. 3E). These observations, combined with our pre-

vious mass spectrometry data, demonstrate that truncated ADPH can correctly localize to CLDs and that CLDs containing truncated ADPH can undergo secretion as milk fat globules. We have shown previously that ADPH forms a stable complex with xanthine oxidoreductase and butyrophilin on milk fat globule membranes (32). Thus, the detection of truncated ADPH on milk fat globule membranes (data not shown) is consistent with the possibility that it may form similar functional interactions with these molecules and consequently contribute to CLD secretion, possibly explaining the relatively modest reduction in the milk fat content of Δ2,3 ADPH mice. Although the presence of a functionally active truncated form of ADPH may also explain the limited phenotype observed in liver and fibroblasts of Δ2,3 ADPH mice (25, 31), preliminary RT-PCR data using primers targeted to exons 4 and 5 in the liver detected no truncated ADPH transcripts compared with the mammary gland (data not shown). It is currently unclear whether this is attributable to tissue-specific transcriptional regulation or to the known instability of RNA isolated from the liver.

Our current findings are consistent with previous studies showing a close correlation between full-length ADPH expression and CLD accumulation in differentiating secretory epithelial cells of WT mice (5, 36). However, truncated ADPH does not appear to contribute to this process in Δ2,3 ADPH mice, as only limited amounts of truncated ADPH are present in their mammary glands before parturition, despite the presence of numerous large CLDs in their secretory epithelial cells during late pregnancy. Moreover, these large CLDs fail to show significant ADPH staining with antibodies specific to either N-terminal or C-terminal sequences of mouse ADPH. In contrast, observations that TIP47 levels increase in mammary glands of Δ2,3 ADPH mice during mammary gland differentiation, and that large TIP47-postive CLDs are present in secretory epithelial cells of these mice during late pregnancy, suggest that it many mediate CLD accumulation in differentiating Δ2,3 ADPH mammary glands. These data corroborate recent studies demonstrating that TIP47 localizes to CLDs in embryonic fibroblasts from Δ2,3 ADPH mice (25) and are consistent with the hypothesis that it contributes to CLD formation when ADPH is lacking (25). However, the dramatic decline in mammary gland TIP47 levels after parturition, and the reduction of TIP47 staining of CLDs in secretory epithelial cells of lactating Δ2,3 ADPH mice, raise questions about whether it plays a similar role in the formation and secretion of milk lipids during lactation. Indeed, the reciprocal relationship between TIP47 and truncated ADPH levels observed in differentiating and lactating Δ2,3 ADPH mammary tissues suggests that CLD accumulation in these mice may involve independent and stage-specific actions of both molecules, with TIP47 regulating CLD accumulation in differentiating Δ2,3 ADPH mammary glands and truncated ADPH regulating CLD formation and secretion in lactating mammary glands.

Studies by Sztalryd et al. (25) in embryonic fibroblasts from Δ2,3 ADPH demonstrated that the loss of ADPH resulted in apparent compensatory increases in transcript and protein levels of TIP47, which suggested that the expression of these proteins may be inversely related. Consistent with this concept, we found that TIP47 levels in Δ2,3 ADPH mammary glands were increased over those of WT glands during the period of mammary gland differentiation, when the truncated form of ADPH was not detectable, and that as the levels of truncated ADPH increased during lactation, the levels of TIP47 in Δ2,3 ADPH mammary glands declined. In contrast to embryonic fibroblasts, transcript levels of TIP47 in Δ2,3 ADPH mammary glands did not differ from those in WT mammary glands, which suggests that if functional compensation exists between ADPH and TIP47 in the mammary gland, it is regulated by posttranscriptional mechanisms. However, it is important to note that in WT mammary glands, both ADPH and TIP47 levels increase during lactation. Thus, functional compensation between these proteins may not be a general property of all tissues and may be influenced by both developmental and tissue-specific factors.

In summary, our results show that lactating mammary glands of Δ2,3 ADPH mice produce an N-terminally truncated form of ADPH with the necessary expression and localization properties to function in the formation and secretion of milk lipids. Although previous studies have documented that the N-terminal region is not required for targeting ADPH to CLDs in transient transfection models (33, 37), our study provides the first in vivo evidence that the N-terminal region of ADPH may not be required for its activity. Our data also provide in vivo evidence for the hypothesis that TIP47 can compensate for the loss of ADPH in CLD accumulation in differentiating mammary glands. Although detailed understanding of the physiological functions of ADPH and TIP47 in milk lipid formation and secretion will require complete functional knockouts of one or both molecules, Δ2,3 ADPH mice provide a potentially useful model to identify the molecular interactions that govern interactions between ADPH and other molecules involved in milk lipid formation.

This research was supported by National Institutes of Health Grants RO1 HD-045965 and PO1 HD-38129 to J.L.M. C.A.P. was supported by National Research Service Award Postdoctoral Fellowship HD044359. T.D.R. is a United Negro College Fund Merck Graduate Science Research Fellow. The authors thank Dr. Gregory Shipley at the University of Texas Health Sciences Center for QRT-PCR assistance.

REFERENCES

1. Londos, C., D. L. Brasaemle, C. J. Schultz, J. P. Segrest, and A. R. Kimmel. 1999. Perilipins, ADRP, and other proteins that associate with intracellular neutral lipid droplets in animal cells. *Semin. Cell Dev. Biol.* **10:** 51–58.
2. Murphy, D. J. 2001. The biogenesis and functions of lipid bodies in animals, plants and microorganisms. *Prog. Lipid Res.* **40:** 325–438.
3. Mather, I. H., and T. W. Keenan. 1998. Origin and secretion of milk lipids. *J. Mammary Gland Biol. Neoplasia.* **3:** 259–273.

4. McManaman, J. L., M. E. Reyland, and E. C. Thrower. 2006. Secretion and fluid transport mechanisms in the mammary gland: comparisons with the exocrine pancreas and the salivary gland. *J. Mammary Gland Biol. Neoplasia.* **11:** 249–268.
5. Russell, T. D., C. A. Palmer, D. J. Orlicky, A. Fischer, M. C. Rudolph, M. C. Neville, and J. L. McManaman. 2007. Cytoplasmic lipid droplet accumulation in developing mammary epithelial cells: roles of adipophilin and lipid metabolism. *J. Lipid Res.* **48:** 1463–1475.
6. Londos, C., D. L. Brasaemle, J. Gruia-Gray, D. A. Servetnick, C. J. Schultz, D. M. Levin, and A. R. Kimmel. 1995. Perilipin: unique proteins associated with intracellular neutral lipid droplets in adipocytes and steroidogenic cells. *Biochem. Soc. Trans.* **23:** 611–615.
7. Brasaemle, D. L., T. Barber, N. E. Wolins, G. Serrero, E. J. Blanchette-Mackie, and C. Londos. 1997. Adipose differentiation-related protein is an ubiquitously expressed lipid storage droplet-associated protein. *J. Lipid Res.* **38:** 2249–2263.
8. Heid, H. W., R. Moll, I. Schwetlick, H. R. Rackwitz, and T. W. Keenan. 1998. Adipophilin is a specific marker of lipid accumulation in diverse cell types and diseases. *Cell Tissue Res.* **294:** 309–321.
9. Carroll, K. S., J. Hanna, I. Simon, J. Krise, P. Barbero, and S. R. Pfeffer. 2001. Role of Rab9 GTPase in facilitating receptor recruitment by TIP47. *Science.* **292:** 1373–1376.
10. Bohn, H., W. Kraus, and W. Winckler. 1983. Purification and characterization of two new soluble placental tissue proteins (PP13 and PP17). *Oncodev. Biol. Med.* **4:** 343–350.
11. Than, N. G., B. Sumegi, G. N. Than, G. Kispal, and H. Bohn. 1998. Cloning and sequence analysis of cDNAs encoding human placental tissue protein 17 (PP17) variants. *Eur. J. Biochem.* **258:** 752–757.
12. Diaz, E., and S. R. Pfeffer. 1998. TIP47: a cargo selection device for mannose 6-phosphate receptor trafficking. *Cell.* **93:** 433–443.
13. Miura, S., J. W. Gan, J. Brzostowski, M. J. Parisi, C. J. Schultz, C. Londos, B. Oliver, and A. R. Kimmel. 2002. Functional conservation for lipid storage droplet association among Perilipin, ADRP, and TIP47 (PAT)-related proteins in mammals, Drosophila, and Dictyostelium. *J. Biol. Chem.* **277:** 32253–32257.
14. Than, N. G., B. Sumegi, S. Bellyei, T. Berki, G. Szekeres, T. Janaky, A. Szigeti, H. Bohn, and G. N. Than. 2003. Lipid droplet and milk lipid globule membrane associated placental protein 17b (PP17b) is involved in apoptotic and differentiation processes of human epithelial cervical carcinoma cells. *Eur. J. Biochem.* **270:** 1176–1188.
15. Wu, C. C., K. E. Howell, M. C. Neville, J. R. Yates, 3rd, and J. L. McManaman. 2000. Proteomics reveal a link between the endoplasmic reticulum and lipid secretory mechanisms in mammary epithelial cells. *Electrophoresis.* **21:** 3470–3482.
16. Liu, P., Y. Ying, Y. Zhao, D. I. Mundy, M. Zhu, and R. G. Anderson. 2004. Chinese hamster ovary K2 cell lipid droplets appear to be metabolic organelles involved in membrane traffic. *J. Biol. Chem.* **279:** 3787–3792.
17. Jiang, H. P., and G. Serrero. 1992. Isolation and characterization of a full-length cDNA coding for an adipose differentiation-related protein. *Proc. Natl. Acad. Sci. USA.* **89:** 7856–7860.
18. Steiner, S., D. Wahl, B. L. Mangold, R. Robison, J. Raymackers, L. Meheus, N. L. Anderson, and A. Cordier. 1996. Induction of the adipose differentiation-related protein in liver of etomoxir-treated rats. *Biochem. Biophys. Res. Commun.* **218:** 777–782.
19. Gao, J., H. Ye, and G. Serrero. 2000. Stimulation of adipose differentiation related protein (ADRP) expression in adipocyte precursors by long-chain fatty acids. *J. Cell. Physiol.* **182:** 297–302.
20. Vosper, H., L. Patel, T. L. Graham, G. A. Khoudoli, A. Hill, C. H. Macphee, I. Pinto, S. A. Smith, K. E. Suckling, C. R. Wolf, et al. 2001. The peroxisome proliferator-activated receptor delta promotes lipid accumulation in human macrophages. *J. Biol. Chem.* **276:** 44258–44265.
21. Buechler, C., M. Ritter, C. Q. Duong, E. Orso, M. Kapinsky, and G. Schmitz. 2001. Adipophilin is a sensitive marker for lipid loading in human blood monocytes. *Biochim. Biophys. Acta.* **1532:** 97–104.
22. Gupta, R. A., J. A. Brockman, P. Sarraf, T. M. Willson, and R. N. DuBois. 2001. Target genes of peroxisome proliferator-activated receptor gamma in colorectal cancer cells. *J. Biol. Chem.* **276:** 29681–29687.
23. Exil, V. J., R. L. Roberts, H. Sims, J. E. McLaughlin, R. A. Malkin, C. D. Gardner, G. Ni, J. N. Rottman, and A. W. Strauss. 2003. Very-long-chain acyl-coenzyme A dehydrogenase deficiency in mice. *Circ. Res.* **93:** 448–455.
24. Tansey, J. T., C. Sztalryd, J. Gruia-Gray, D. L. Roush, J. V. Zee, O. Gavrilova, M. L. Reitman, C. X. Deng, C. Li, A. R. Kimmel, et al. 2001. Perilipin ablation results in a lean mouse with aberrant adipocyte lipolysis, enhanced leptin production, and resistance to diet-induced obesity. *Proc. Natl. Acad. Sci. USA.* **98:** 6494–6499.
25. Sztalryd, C., M. Bell, X. Lu, P. Mertz, S. Hickenbottom, B. H. Chang, L. Chan, A. R. Kimmel, and C. Londos. 2006. Functional compensation for adipose differentiation-related protein (ADFP) by Tip47 in an ADFP null embryonic cell line. *J. Biol. Chem.* **281:** 34341–34348.
26. Allen, J. C., R. P. Keller, P. C. Archer, and M. C. Neville. 1991. Studies in human lactation. VI. Milk composition and daily secretion rates of macronutrients in the first year of lactation. *Am. J. Clin. Nutr.* **54:** 69–80.
27. Schwertfeger, K. L., J. L. McManaman, C. A. Palmer, M. C. Neville, and S. M. Anderson. 2003. Expression of constitutively activated Akt in the mammary gland leads to excess lipid synthesis during pregnancy and lactation. *J. Lipid Res.* **44:** 1100–1112.
28. Neville, M. C., and C. W. Daniel. 1987. The Mammary Gland: Development, Regulation and Function. Plenum Press, New York.
29. Anderson, S. M., M. C. Rudolph, J. L. McManaman, and M. C. Neville. 2007. Key stages in mammary gland development. Secretory activation in the mammary gland: it's not just about milk protein synthesis! *Breast Cancer Res.* **9:** 204–217.
30. Hollmann, K. H. 1974. Cytology and fine structure of the mammary gland. *In* Lactation. B. L. Larson and V. R. Smith, editors. Academic Press, New York. 3–95.
31. Chang, B. H., L. Li, A. Paul, S. Taniguchi, V. Nannegari, W. C. Heird, and L. Chan. 2006. Protection against fatty liver but normal adipogenesis in mice lacking adipose differentiation-related protein. *Mol. Cell. Biol.* **26:** 1063–1076.
32. McManaman, J. L., C. A. Palmer, R. M. Wright, and M. C. Neville. 2002. Functional regulation of xanthine oxidoreductase expression and localization in the mouse mammary gland: evidence of a role in lipid secretion. *J. Physiol.* **545:** 567–579.
33. McManaman, J. L., W. Zabaronick, J. Schaack, and D. J. Orlicky. 2003. Lipid droplet targeting domains of adipophilin. *J. Lipid Res.* **44:** 668–673.
34. Lu, X., J. Gruia-Gray, N. G. Copeland, D. J. Gilbert, N. A. Jenkins, C. Londos, and A. R. Kimmel. 2001. The murine perilipin gene: the lipid droplet-associated perilipins derive from tissue-specific, mRNA splice variants and define a gene family of ancient origin. *Mamm. Genome.* **12:** 741–749.
35. Kozak, M. 1987. At least six nucleotides preceding the AUG initiator codon enhance translation in mammalian cells. *J. Mol. Biol.* **196:** 947–950.
36. Rudolph, M. C., J. L. McManaman, T. Phang, T. Russell, D. J. Kominsky, N. J. Serkova, T. Stein, S. M. Anderson, and M. C. Neville. 2007. Metabolic regulation in the lactating mammary gland: a lipid synthesizing machine. *Physiol. Genomics.* **28:** 323–336.
37. Targett-Adams, P., D. Chambers, S. Gledhill, R. G. Hope, J. F. Coy, A. Girod, and J. McLauchlan. 2003. Live cell analysis and targeting of the lipid droplet-binding adipocyte differentiation-related protein. *J. Biol. Chem.* **278:** 15998–16007.